JACS
JOURNAL OF THE AMERICAN CHEMICAL SOCIETY
Article
pubs.acs.org/JACS

A New View of Electrochemistry at Highly Oriented Pyrolytic Graphite

Anisha N. Patel,[†] Manon Guille Collignon,[†,+] Michael A. O'Connell,[†] Wendy O. Y. Hung,[†] Kim McKelvey,[†,‡] Julie V. Macpherson,[†] and Patrick R. Unwin*[,†]

[†]Department of Chemistry and [‡]MOAC Doctoral Training Centre, University of Warwick, Coventry CV4 7AL, U.K.

Supporting Information

ABSTRACT: Major new insights on electrochemical processes at graphite electrodes are reported, following extensive investigations of two of the most studied redox couples, $Fe(CN)_6^{4-/3-}$ and $Ru(NH_3)_6^{3+/2+}$. Experiments have been carried out on five different grades of highly oriented pyrolytic graphite (HOPG) that vary in step-edge height and surface coverage. Significantly, the same electrochemical characteristic is observed on all surfaces, independent of surface quality: initial cyclic voltammetry (CV) is close to reversible on freshly cleaved surfaces (>400 measurements for $Fe(CN)_6^{4-/3-}$ and >100 for $Ru(NH_3)_6^{3+/2+}$), in marked contrast to previous studies that have found very slow electron transfer (ET) kinetics, with an interpretation that ET only occurs at step edges. Significantly, high spatial resolution electrochemical imaging with scanning electrochemical cell microscopy, on the highest quality mechanically cleaved HOPG, demonstrates definitively that the pristine basal surface supports fast ET, and that ET is not confined to step edges. However, the history of the HOPG surface strongly influences the electrochemical behavior. Thus, $Fe(CN)_6^{4-/3-}$ shows markedly diminished ET kinetics with either extended exposure of the HOPG surface to the ambient environment or repeated CV measurements. *In situ* atomic force microscopy (AFM) reveals that the deterioration in apparent ET kinetics is coupled with the deposition of material on the HOPG electrode, while conducting-AFM highlights that, after cleaving, the local surface conductivity of HOPG deteriorates significantly with time. These observations and new insights are not only important for graphite, but have significant implications for electrochemistry at related carbon materials such as graphene and carbon nanotubes.

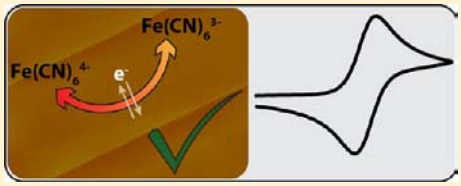

INTRODUCTION

The electrochemical characteristics of highly oriented pyrolytic graphite (HOPG) and related materials are presently attracting considerable attention.[1] In part, this has been driven by a desire to identify similarities and differences in the electrochemistry of HOPG, carbon nanotubes (CNTs),[1e−h] and graphene,[1a,2] which share the same basic sp^2 carbon structural motif, and are attracting huge interest for electrochemically related applications. Furthermore, knowledge of the intrinsic electrochemical properties of HOPG and graphite impacts our understanding of a diversity of processes, from carbon surface functionalization[3] to (electro)catalysis.[4] Moreover, the basal surface of HOPG has proven popular as an electrode support for investigations of heterogeneous metal nucleation and electrodeposition,[5] for model studies of nanoparticle (NP) electrocatalysts,[6] and the creation of nanostructured interfaces for electrochemistry, sensing, and biosensing.[5b,7] In all of these areas, a true understanding of the electrochemistry of the basal surface of HOPG is crucial for the rational design of functionalized interfaces, electrochemical sensors, and electrocatalysts.

A large body of work has suggested that the basal surface of HOPG is characterized by rather poor electrode kinetics, compared to edge plane graphite, for a wide range of redox couples, including classical outer-sphere and inner-sphere couples.[8] Indeed, until recently, the traditional consensus was that the basal surface of HOPG had very low activity[8d] or even no electroactivity,[1g,8a,f,g,9] with the step edges intersecting the basal surface providing essentially all of the sites for electron transfer (ET) for a range of redox couples.[1e−h,8a,f−i] However, even within this body of work there are significant differences in the behavior reported for some redox couples. Furthermore, recent microscopic and nanoscopic studies challenge this model and suggest that the pristine basal surface of HOPG has significant ET activity.[1d,10] As a consequence, and given the prominence of HOPG as an important electrode material, we have undertaken a thorough study of its electrochemical and surface properties (*vide infra*), with the aim of providing a coherent view of the field. We deduce that pristine, freshly cleaved HOPG actually has considerable activity as an electrode material, but complex surface effects operate that may alter its behavior. Importantly, we propose a model which is self-consistent from the nanoscale to macroscale and which can be tested directly at this range of length scales.

Claims about the inactivity of basal plane HOPG have, in some cases, led to further speculation about the sites of ET on CNTs[1g,8g,11] and graphene.[1a,12] Specifically, it has been proposed that interfacial ET only occurs at edge-plane like sites in multi-walled CNTs and at the open ends of single-

Received: August 30, 2012
Published: November 12, 2012

walled and multi-walled CNTs,[1g,8f,g,13] or at the graphene edge.[12] In contrast, fast (often reversible) electrochemistry is evident in studies of pristine, well-characterized single-walled carbon nanotubes (SWNTs) grown by chemical vapor deposition,[14] and at mechanically exfoliated graphene,[15] suggesting that ET occurs readily at the interface between sp^2 carbon and electrolyte solution. This provides a further impetus to understand HOPG electrochemistry more fully, not least because SWNT network electrodes and single nanotube devices[13,14a−h,16] show unprecedented limits of detection in voltammetric analysis (orders of magnitude better than other common carbon materials and d-metals).[1f]

A wide range of peak-to-peak separation (ΔE_p) values in cyclic voltammetry (CV) measurements of $Fe(CN)_6^{4-/3-}$ (typical scan rates 0.1−1 V s^{-1}; although occasionally higher[8d])) have been found on the cleaved basal surface, in the range from 58 mV (essentially reversible) to 1.5 V.[1g,8c,f,9c,17] This corresponds to effective standard heterogeneous ET rate constants, k_o (in terms of the net current response for the entire surface), of at least 5−8 orders of magnitude, from less than 10^{-9} cm s^{-1} [1g,9c] or 10^{-6} cm s^{-1} [8d,e] to >0.1 cm s^{-1} (i.e., reversible on the CV time scale under conditions of planar diffusion).[1e−h,18] By implication, a similar change in the magnitude of surface defect (step) coverage, from one cleave of HOPG to another, would reasonably be expected within the bounds of a step defect-driven model of HOPG electrode activity. This is not evident based on current knowledge of step-edge density on freshly cleaved HOPG. Indeed, early scanning tunneling microscopy of the basal surface of HOPG revealed step-edge densities in the range of 1−10%,[19] and this appears to be a generally accepted range, with the step-edge density depending on the source of HOPG and cleavage method.[20] We provide detailed analysis of this aspect herein. Other approaches for probing HOPG surface quality which have been complemented with CV measurements have included capacitance measurements,[8b,d,21] complementary microscopy and spectroscopy studies,[8a,20−22] and anthraquinone disulfonate adsorption, which was proposed to serve as an indirect marker of step (defect) density.[8d]

Recent advances in electrochemical imaging have facilitated localized investigations of HOPG in defined locations and at high spatial resolution.[1d,10] Such studies allow local electrochemical measurements to be correlated directly with the corresponding surface structure. We recently used scanning electrochemical cell microscopy (SECCM) to investigate the basal surface of HOPG with a spatial resolution an order of magnitude smaller than the characteristic step spacing.[1d] Moreover, SECCM allowed the location of the measurements (step edge or basal surface) to be determined unambiguously. We found the ET kinetics for both $Fe(CN)_6^{4-/3-}$ and $Ru(NH_3)_6^{3+/2+}$ to be close to reversible (k_o > 0.1 cm s^{-1}), although we noted that the $Fe(CN)_6^{4-/3-}$ response diminished significantly with time during the course of recording an image. These studies built on earlier investigations with the scanning micropipet contact method (SMCM)[10c] which also indicated that the basal plane of HOPG was active toward the electrochemistry of iron complexes, including $Fe(CN)_6^{4-/3-}$, provided that measurements were made rapidly on freshly cleaved surfaces. A similar conclusion was reached for positively charged redox-active complexes, including $Ru(NH_3)_6^{3+/2+}$, by slowing down diffusion to the HOPG surface using a Nafion film.[10a] Frederix et al.[10b] and Demaille et al.[10d] also recently used different variants of scanning electrochemical microscopy and atomic force microscopy (SECM-AFM)[23] to show that the HOPG basal surface was highly electrochemically active, although they also noted sometimes that step edges showed slightly enhanced activity. Notably, Frederix found that the kinetics for $Ru(NH_3)_6^{3+/2+}$ were just as facile on the basal surface of HOPG as on template-stripped Au and Pt, and up to 2 orders of magnitude faster than measured in early CV studies.[8c] It was, however, observed that the ET kinetics at the basal surface depreciated over extended time.

To summarize: there are significant differences between the results obtained from microscale and nanoscale electrochemical measurements, on the one hand, and macroscale investigations, on the other hand. Moreover, at the macroscale, significant differences are evident in electrochemical behavior of apparently similar HOPG.[7g,8f,h,20,24] Further surprising is that studies purporting to show that the basal surface of HOPG supports only sluggish or no ET[7g,8f,h,20,24] have been obtained on HOPG with very different surface quality (*vide infra*), and might have been expected to show contrasting behavior within the framework of a defect-driven activity model. Given the importance of HOPG as an electrode material, as highlighted herein, and its recent prominence as a comparator for graphene studies,[1a,15,25] the studies in this paper aim to resolve and explain the issues highlighted. Our investigations have been carried out intermittently for a period of more than 6 years, on more than 25 HOPG samples, with cleavage of the surface and voltammetry performed independently by four different people. We have considered ambient conditions, since these have been used in all previous electrochemical studies. Initially, we focused on the oxidation of $Fe(CN)_6^{4-}$ (CV measurements on >400 freshly cleaved surfaces), as most previous studies have been carried out with this electrode reaction, but included further studies of $Ru(NH)_3^{3+}$ reduction (measurements on >100 freshly cleaved surfaces), given the discrepancies in ET kinetics alluded to above.[3c,6b,25] We have examined four commercially available HOPG samples: ZYA, ZYH, SPI-1, and SPI-2 (all from SPI supplies, Aztech Trading, UK), the first three of which have been employed in previous electrochemical studies.[7g,8f,h,20,24] We were also able to study high-quality unclassified HOPG.

We show unequivocally that freshly cleaved pristine HOPG is much more electrochemically active than previously considered; however, the HOPG basal surface is shown to readily passivate in a number of ways. A particularly important observation is that the $Fe(CN)_6^{4-/3-}$ couple blocks and modifies the surface of HOPG during voltammetry, making this couple unsuitable for "validation experiments",[3,19,20] and for the assessment of electrode kinetics.[8f,h] We see consistent behavior at both the macroscale and nanoscale, and our studies provide a self-consistent and new view of HOPG electrochemistry, with significant implications for studying and understanding electrochemistry at related sp^2 materials.

EXPERIMENTAL SECTION

Materials and Solutions. All chemicals were used as received. Aqueous solutions were prepared using high purity water (Milli-Q, Millipore) with a resistivity of ca. 18.2 MΩ cm at 25 °C. For voltammetry, solutions typically contained either 1 mM potassium ferrocyanide trihydrate ($K_4Fe(CN)_6{\cdot}3H_2O$; 99.99%, Sigma-Aldrich or 99%, Fisher Scientific) in either 0.1 or 1 M potassium chloride (KCl; Fisher Scientific, analytical grade) as supporting electrolyte, or 1 mM hexaaminеruthenium(III) chloride ($Ru(NH_3)_6Cl_3$; 99.00% purity, Strem Chemicals) in either 0.5 or 1 M KCl. However, some $Fe(CN)_6^{4-}$ oxidation experiments considered concentrations up to 10

Table 1. Characterization of HOPG Properties and Topography

	ZYA	SPI-1	ZYH	SPI-2	AM[d]
mosaic spread[a]	0.4° ± 0.1°	0.4° ± 0.1°	3.5° ± 1.5°	0.8° ± 0.2°	n/a
step density range (μm μm^{-2}) from AFM	0.1−0.7	0.3−3.6	0.5−2.3	1−3.5	0.003−0.12
mean step density (μm μm^{-2}) from AFM[b]	0.5 ± 0.1 (N = 15)	1.5 ± 0.2 (N = 14)	1.2 ± 0.6 (N = 10)	2.1 ± 0.9 (N = 10)	0.02 ± 0.02 (N = 20)
average step-edge coverage on basal plane	0.3% (range 0.03−1%)	1.8% (range 0.5−3.4%)	0.8% (range 0.2−2.1%)	2.2% (range 0.6−6.7%)	0.09% (range 0.006−0.48%)
size (mm)	12 × 12 × 2	10 × 10 × 2	12 × 12 × 2	10 × 10 × 2	varied
capacitance (μF cm^{-2})[b,c]	2.0 ± 0.3 (range 1.7−2.8) (N = 10)	2.9 ± 1.2 (range 2.0−3.8) (N = 10)	–	–	2.4 ± 1.5 (range 0.7−7.4) (N = 20)

[a]From www.spi2.com. The mosaic spread describes how ordered a sample is by providing the average angle of deviation of grains from the perpendicular axis. [b]For image analysis and capacitance measurements, N refers to the number of cleaved surfaces investigated. Errors are 1 standard deviation. [c]Measured at 0.05 V vs Ag/AgCl (1.0 M KCl). [d]AM was mechanically cleaved and other samples were cleaved using Scotch tape.

mM, and some control experiments were carried out with 0.1 M phosphate buffer (pH 7.2). For silver electrodeposition on HOPG, solutions contained 1 mM silver nitrate ($AgNO_3$; AnalaR) in 1 M potassium nitrate (KNO_3; Fisher Scientific). All solutions were freshly prepared on the day of the experiments and stored in the dark when not in use. Measurements were made at ambient temperature (typically 22 ± 2 °C) in air-conditioned rooms.

Four different grades of commercially available HOPG were employed: SPI-1, SPI-2, ZYA, and ZYH, all from SPI supplies (Aztech Trading, UK, http://www.2spi.com). SPI-1 and SPI-2 are SPI brand samples; ZYA and ZYH are GE Advanced Ceramics brand samples. We also had access to a high-quality, but ungraded, HOPG sample, originating from Dr. A. Moore, Union Carbide (now GE Advanced Ceramics), which was kindly provided by Prof. R. L. McCreery (University of Alberta, Canada). Hereafter, we refer to this as HOPG (AM). Table 1 contains key information on the properties and topography of these materials. Note that, as discussed below, the four commercial samples were cleaved with Scotch tape to reveal a fresh surface for study, while HOPG (AM) was subjected to mechanical cleavage.

Electrical Contact to HOPG. The samples were electrically contacted using one of two different supports: either (i) a printed circuit board (PCB), with an underlying electrical contact; or (ii) a silicon wafer, which was coated with a thermally evaporated layer of chromium (10 nm) followed by a layer of gold (100 nm) to create an electrical contact. With the PCB, HOPG was adhered onto a square section using double sided adhesive tape designed for securing samples for AFM. Silver paint (Electrodag, Agar Scientific) was gently applied to the edge of the HOPG and the PCB to make an electrical connection. Finally, tinned copper wire was soldered to the PCB in order to make an external electrical contact. In the case of the silicon wafer, HOPG was adhered onto the gold layer using Acheson Electrodag (1415M, Agar Scientific). An external electrical contact was created by lowering a metal pin onto the gold surface using a micropositioner. This method also enabled samples to be secured for AFM and conducting AFM (C-AFM); see below.

Macroscale Electrochemistry. CV and chronoamperometry (CA) measurements were carried out in a three-electrode configuration using a potentiostat (CH Instruments model 750A, Austin, TX). A silver/silver chloride (Ag/AgCl) wire in KCl (0.1, 0.5 or 1 M as specified) served as the reference electrode. All potentials are quoted against the reference electrode employed (*vide infra*). The reference electrode was used in conjunction with a Pt gauze auxiliary electrode. For time effect studies the reference electrode was a Ag/AgCl wire placed inside a capillary which was fitted with an agar plug and filled with 1 M KCl.[26] Capacitance measurements (Table 1) were made by simple CV measurements in 1 M KCl supporting electrolyte, as outlined in Supporting Information, section S1.

Cells for Voltammetry on HOPG. One of the issues for voltammetric measurements at basal surface HOPG is how to present the material in an electrochemical cell, so that only the basal surface is exposed and there is no strain or distortion of the sample. HOPG is rather unusual in that it cannot readily be encapsulated for study, nor can it be cycled to extreme potentials for cleaning without disrupting the surface[27] and promoting ion intercalation.[28] For the studies reported herein, voltammetry was performed on freshly cleaved HOPG surfaces initially using a droplet arrangement.[14a,29] This avoided any possible mechanical strain on the HOPG surface. However, this arrangement was eventually superseded by a small PTFE cell as no difference was seen in voltammetric behavior with the two arrangements, and the PTFE cell was extremely useful for long time tests where more extensive solution evaporation might otherwise have been problematic. It was also essential for measurements where the area of HOPG exposed to solution needed to be known with high precision (e.g., for capacitance measurements), as the cell resulted in a well-defined disk electrode of HOPG of 3 mm diameter. These cells allowed measurements within 1 min of sample cleavage. We also reproduced a reported cell design in which HOPG was secured with pressure applied to an O-ring,[24] but found the response to be sensitive to the amount of pressure applied, with the voltammetry becoming distorted when the sample was increasingly compressed. Full details of the droplet and PTFE cells are given in Supporting Information, section S2. Unless otherwise stated, measurements reported herein generally refer to the PTFE cell arrangement.

The cells utilized had relatively small volume-to-working electrode area ratios, and it was important to assess the extent of any changes in solution composition (including pH) due to electrolysis at the working and auxiliary electrodes. Experiments with pH 7.2 buffered solutions showed similar trends to the experiments reported herein without buffer (see Supporting Information, section S3), indicating that any possible change in solution pH was not an issue for the experiments reported. Furthermore, the change in solution composition was negligible on the time scale and extent of the measurements (*vide infra*). Finally, we also carried out some measurements on freshly cleaved surfaces with a capillary cell,[14b,d] using a glass capillary of ca. 50 μm diameter. In this arrangement the diffusion layer at the working electrode is significantly smaller (by several orders of magnitude) than the height of solution in the capillary so that compositional changes are negligible. We observed similar behavior to that reported herein with the other cell arrangements.

Scanning Electrochemical Cell Microscopy. High-resolution electrochemical imaging[30] was performed on mechanically cleaved HOPG (AM) as described in detail elsewhere.[1d,30] We provide salient details here. A tapered dual-channel glass pipet, with an opening of ca. 350 nm (measured accurately with field-emission scanning electron microscopy (FE-SEM), *vide infra*), was filled with 2 mM $Ru(NH_3)_6^{3+}$ salt (0.1 M KCl) and two Ag/AgCl quasi-reference counter electrodes (QRCEs) (one in each channel). The SECCM instrument comprised of a high-dynamic z-piezoelectric positioner (P-753.3CD LISA, Physik Instrumente), on which the pipet was mounted and a xy-piezoelectric stage (P-622.2CL PIHera, Physik Instrumente) for sample mounting. Contact between the liquid meniscus at the end of the pipet and the HOPG surface produced a positionable and movable nano-electrochemical cell. The pipet itself never touched the sample.

A potential bias applied between the two QRCEs resulted in a conductance current across the meniscus. An oscillation (20 nm peak amplitude, 233.3 Hz herein) imposed on the pipet using the *z*-piezoelectric positioner produced an alternating current (AC) component of the conductance current at the same frequency due to the periodic deformation of the liquid meniscus contact.[30,31] This AC was used as a set-point during scanning so that the tip traced the surface at a constant separation (*vide infra*). The SECCM tip was typically scanned over a 5 μm × 10 μm area of HOPG (AM) at a speed of 0.3 μm s^{-1}, scanning 3 lines per μm and recording a data point every 30.1 ms. This resulted in the acquisition of ca. 1100 points per line and over 16 000 individual measurements in an image. During experiments, the current at the substrate was recorded simultaneously with the *xy* and *z* position of the pipet and the conductance current (both DC and AC components). Data acquisition was achieved using an FPGA card (PCIe-7852R) with a LabView 2011 interface. The contact diameter of the meniscus and the substrate was determined in a previous study to be in the range 220−320 nm,[1d] consistent with a growing body of work which indicates that the meniscus contact is of the order of the diameter of the pipet terminus.[1d,31,32]

HOPG Cleaving. Three procedures were used to reveal a pristine freshly cleaved surface as outlined in full in Supporting Information, section S2: (i) the use of Scotch tape to peel back a layer of HOPG and reveal a fresh surface; (ii) a mechanical cleavage procedure applied parallel to the HOPG surface; and (iii) a mechanical cleavage procedure, as carried out previously,[8d,19] in which a razor blade was used to apply gentle pressure perpendicular to the basal plane, allowing a fresh piece to spontaneously delaminate. The latter was used exclusively for HOPG (AM).

For all methods, the cleaved surface was used to run an experiment only if it appeared "shiny" to the eye (indicating lower step density) and was devoid of any visible macroscopic defects. Surfaces were routinely found to have a relatively low density of steps and low capacitance values, although there was some variation (*vide infra*). For each HOPG sample, where Scotch tape was used, the direction of cleaving was maintained in order to avoid deformation of the surface. If the tape used to remove the outermost layers of the HOPG was not completely covered with HOPG, the procedure was repeated to ensure that no area of the surface was contaminated by adhesive from the tape. The Scotch tape method was used most, as this has been used routinely by others.[1e−h,5a,8a−g,10a,33]

AFM Imaging. AFM images of HOPG topography were recorded in air, using a Bruker Nano Multimode V AFM with Nanoscope V controller, in tapping mode (TM). HOPG step density, extracted from these images, is defined as the length of step edges per unit area (Table 1).[14h]

In situ AFM images were obtained in electrolyte solution, with electrochemical control of the HOPG working electrode (CH Instruments model 750A or 800B potentiostat, Austin, Texas). TM-AFM images were recorded using an Environmental AFM (Enviroscope, Bruker) with Nanoscope IV controller. The PCB-supported HOPG sample was adhered to an Enviroscope fluid cell using adhesive tape. The cell was filled with ca. 4.5 mL of a solution containing either 1 mM $Fe(CN)_6^{4-}$ salt (99.99%) in 1 M KCl, or 1 mM $Ru(NH_3)_6^{3+}$ salt in 0.5 M KCl. The PCB and sides of the HOPG were isolated from solution using a mix of 1:1 super glue and nail varnish. An Ag/AgCl wire served as the reference electrode (in the KCl electrolyte) and a Pt gauze was again used as the auxiliary electrode. Measurements were made with and without nitrogen flow to deaerate the solution with similar results.

Conducting AFM. C-AFM images of HOPG were obtained using a Veeco Multimode V AFM with a conducting module and Nanoscope V controller. In imaging mode, a bias of 20 mV was typically applied to a Pt−Ir-coated Si probe (SCM-PIC, Bruker, quoted nominal radius of curvature ~20 nm) using the controller, with a current-limiting resistor of 1 MΩ in series with the grounded sample; the current output was detected by the controller. Experiments were also made where the tip was held stationary in an area of interest and conductance current−voltage (*i*−*V*) curves recorded. C-AFM was carried out either as soon as possible on freshly cleaved HOPG or as a function of time in air after cleaving (*vide infra*). After measurements, the integrity of all conducting tips was checked by replacing the sample with a new piece of freshly cleaved HOPG surface.

FE-SEM. A Zeiss SUPRA 55 VP field emission scanning electron microscopy with an in-lens detector was used to obtain images of HOPG.

RESULTS AND DISCUSSION

HOPG Surface Topography and Step Density. In order to understand the relationship between the voltammetric behavior of HOPG and surface structure it was important to fully characterize sample topography, particularly since the overwhelming majority of previous voltammetric studies (see Introduction) have suggested that HOPG electroactivity is dominated, or controlled entirely, by step edges (edge planes) with the basal plane providing little or no contribution. Given its use as a flat substrate for imaging nanostructures and biomaterials,[34] there are many AFM images of HOPG in the literature, but only a few studies[21,20,19] have examined HOPG surfaces of different grades in any detail. Here, we investigated the surface topography of four major types of commercially available HOPG and HOPG (AM) in more detail than in any previous study to obtain clear bounds on the step density, which is essential to examine the validity (or otherwise) of the step-active models.[1e−g,5a,8a−g,19,28,33,35] Typical TM-AFM images are shown in Figure 1, and a summary of the data obtained is given in Table 1.

Figure 1 and Table 1 show clearly that mechanically cleaved HOPG (AM), closely followed by Scotch tape-cleaved ZYA-grade HOPG, provide by far the most superior surfaces in terms of low step density. The other grades of HOPG show increasing step densities in the order ZYH, SPI-1, and SPI-2.

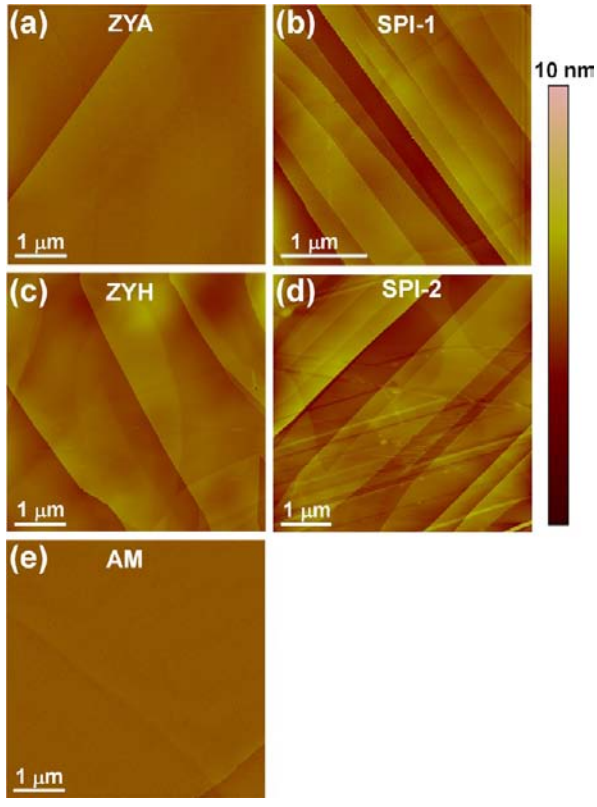

Figure 1. TM-AFM topography images of freshly cleaved HOPG: (a) ZYA, (b) SPI-1, (c) ZYH, (d) SPI-2 grades, and (e) AM.

dx.doi.org/10.1021/ja308615h | J. Am. Chem. Soc. 2012, 134, 20117−20130

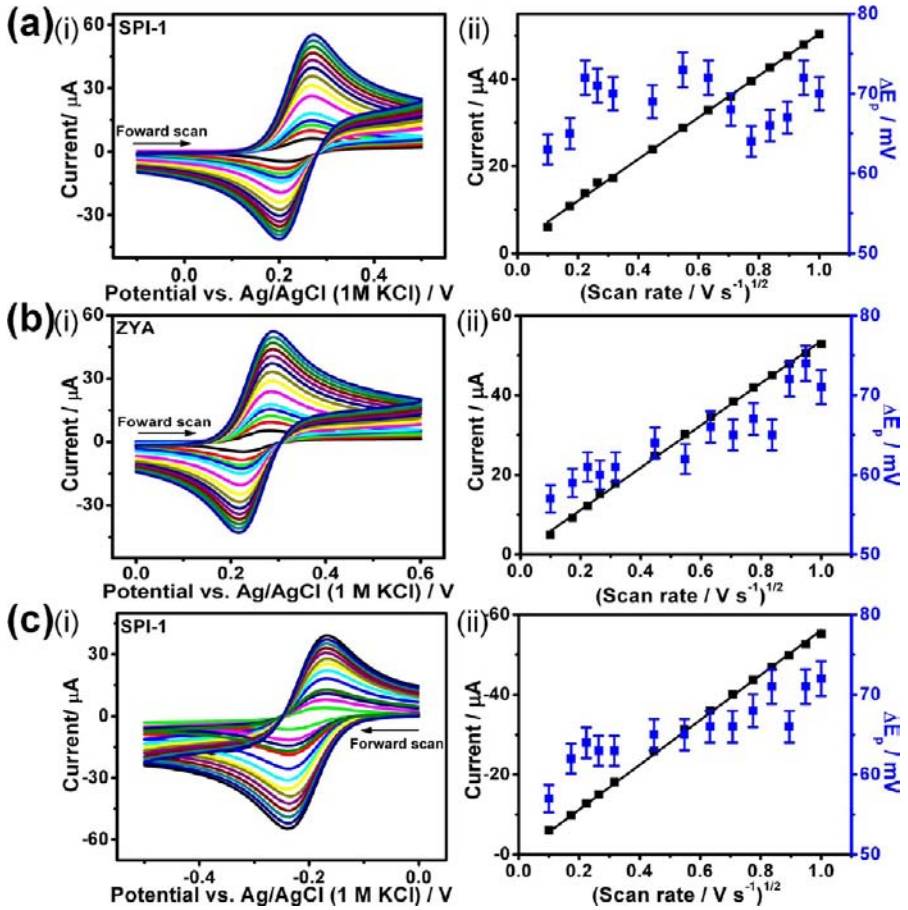

Figure 2. CVs at a range of scan rates for the oxidation of 1 mM $Fe(CN)_6^{4-}$ (99.99%) in 1 M KCl on (a) SPI-1 and (b) ZYA HOPG. (c) CVs for the reduction of 1 mM $Ru(NH_3)_6^{3+}$ in 1 M KCl on HOPG (SPI-1). In all figures labeled (i) the scan rates are as follows: 0.01, 0.03, 0.05, 0.07, 0.1, 0.2, 0.3, 0.4, 0.5, 0.6, 0.7, 0.8, 0.9, 1 V s^{-1}. The corresponding analyses of peak current (i_p) and peak-to-peak separation (ΔE_p) as a function of (scan rate)$^{1/2}$ are shown in (ii). Each CV shown was run on a freshly cleaved surface.

Notably, SPI-1 grade, which has been used extensively for CV measurements,[1c,4a,6b−d,32] shows a much higher step density than ZYA-grade HOPG, even though ZYA and SPI-1 HOPG exhibit a similar mosaic spread. Surprisingly, although ZYH grade appeared to be roughest "to the eye", the cleaved surface was found to have a reasonably low step density.

Given that the layer separation in HOPG is 0.335 nm,[19,23] the AFM images were used to deduce step heights in terms of the number of graphite layers, as reported in Supporting Information, section S4. This analysis shows that most grades of HOPG (except ZYH and SPI-2) exhibit mainly monolayer and bilayer steps. Using the AFM images, we also calculated the fraction of the basal surface occupied by edge plane-like sites. These data are summarized in Table 1. From 69 images across five different grades of HOPG, one can see that the average step-edge coverage varies significantly across the different grades, and also that within a grade, the range (from image to image on a particular surface) can vary by an order of magnitude. Thus, while the HOPG samples used herein provide a set of basal surfaces with different edge plane densities to test the premise that edge planes alone are responsible for the electroactivity of HOPG, our detailed analysis immediately raises questions about the validity of the step-edge active model for two significant reasons. First, previous work[8a−e,20]—highlighted in the Introduction—has found that the standard rate constants of the $Fe(CN)_6^{4-/3-}$ couple, spans a factor of ca. 10^5−10^8, yet step densities,[5h,19−21] including herein across five grades of HOPG, only span a maximum range of 10^2. Second, while studies of different grades of HOPG in one laboratory apparently show different ET kinetics,[8d,21] investigations of different HOPG grades (evidently of widely variable quality based on the data herein) in different laboratories show similar slow ET kinetics.[7g,8f,h,20,24] This appears contradictory for a step-edge model of HOPG activity.

For the commercial samples, cleaved by Scotch tape, it was found that as a particular (new) HOPG sample was cleaved, the step density and step heights tended, very gradually, to become larger. This was consistent with technical information which recommends that the last 1 mm of a sample (i.e., half the initial sample) is discarded, since it comprises the "base layer" in which the mosaic spread is much higher than the "top working layer".[36] We followed this advice for the electrochemical measurements reported.

The AFM analysis of surface quality was supported by capacitance measurements of SPI-1, ZYA and HOPG (AM) (see Supporting Information, section S1). ZYA yielded a capacitance value of 2.0 ± 0.3 μF cm^{-2} (ranging between 1.7 and 2.8 μF cm^{-2}), consistent with the measurements of McCreery et al. on this material.[8d,21] Moreover, the lower capacitance values measured on ZYA-grade HOPG are in agreement with the lowest reported for low defect HOPG in early work (1.9 μF cm^{-2})[8b] for which very large ΔE_p (>700 mV at 0.2 V s^{-1}) was seen for $Fe(CN)_6^{4-/3-}$. On the other hand,

dx.doi.org/10.1021/ja308615h | J. Am. Chem. Soc. 2012, 134, 20117−20130

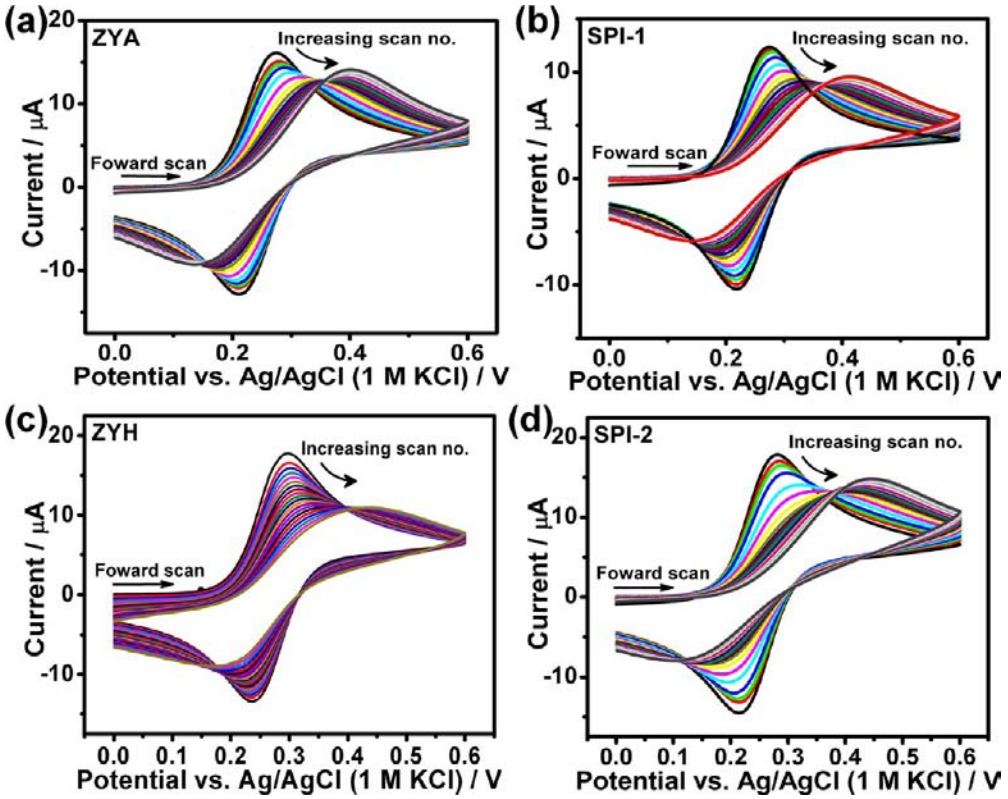

Figure 3. Repeat CVs for the oxidation of 1 mM $Fe(CN)_6^{4-}$ (1 M KCl), run at 0.1 V s^{-1} on (a) ZYA, (b) SPI-1, (c) ZYH, and (d) SPI-2 HOPG. Each cycle was run at 5 min intervals; total of 20 cycles in each case.

SPI-1 HOPG showed a slightly higher mean value and more variation, i.e. 2.9 ± 1.2 μF cm^{-2}, but this is still a reasonably low value in the context of some values reported.[8b,e,37] For example, these values are far superior (lower) compared to those of ZYH-grade HOPG recently reported by Bond and co-workers,[8i] which varied between 3.4 and 7.1 μF cm^{-2} (suggesting surfaces with more defects).[8b,21] Yet, very large ΔE_p (slow kinetics) were still obtained for $Fe(CN)_6^{4-/3-}$ CVs in that work. We can thus be confident that we are working with samples of low step (and defect) density; at least as good as the best reported (for Scotch tape cleaved material), and in many cases better. Mechanically cleaved HOPG (AM) provided the lowest capacitance values (0.7 μF cm^{-2})—which essentially matched the very lowest ever reported for HOPG[7d]—but also occasionally much larger values (7.4 μF cm^{-2}) were seen, leading to an average of 2.4 ± 1.5 μF cm^{-2} (1σ). This is again consistent with the wide range of values reported by McCreery for HOPG (AM), in the range 0.6 and 6.5 μF cm^{-2}.[7d]

FE-SEM was employed to visualize further the step density on ZYA- and SPI-1-grade HOPG over much wider areas, since these were used for most voltammetric studies; see Supporting Information, section S5. This analysis also confirmed that the step density was much lower on ZYA-grade HOPG than SPI-1 grade.

CV Characteristics. *Voltammetry on Freshly Cleaved Surfaces.* We first consider CV measurements as a function of scan rate for SPI-1 and ZYA-grade HOPG. For the plots shown in Figure 2, each CV was run on a freshly cleaved surface. For Figure 2a,b, 1 mM $Fe(CN)_6^{4-/3-}$ (purity 99.99%) in 1 M aqueous KCl was used. Similar data were obtained with 99% purity $Fe(CN)_6^{4-/3-}$. The data shown are entirely representative of measurements carried out on >400 freshly cleaved surfaces with the $Fe(CN)_6^{4-/3-}$ couple, independently by four different people. These measurements show near reversible behavior of the $Fe(CN)_6^{4-/3-}$ couple, for which ΔE_p would be ca. 59 mV[38] (Figure 2a-ii,b-ii)). Although, in principle, one could attempt to analyze the CVs to obtain kinetic information, the ΔE_p values are too close to the reversible limit for this to be meaningful. Furthermore, as shown below, the HOPG surface and the $Fe(CN)_6^{4-/3-}$ couple is complicated by time-dependent heterogeneous surface effects, making a kinetic analysis—that would assume a uniform surface and simple electrochemical process—less than ideal. Evidently, the ΔE_p values are very similar for both types of HOPG despite the very large difference in characteristic step spacing and step coverage (Table 1). The data in Figure 2a-ii,b-ii also clearly show that the (forward) peak current is linear with the square root of scan rate and yielded a diffusion coefficient of 7.3(±0.3) × 10^{-6} cm^2 s^{-1} for $Fe(CN)_6^{4-}$, which is in agreement with literature.[39] The data is in sharp contrast with that reported (*vide supra*) in the past, where values as high as 1.5 V have been observed on samples with low defect density,[1g,8c,d,f,17] but smaller values have also been reported, ranging from ~350 mV[9c] to 58 mV[8c] (indicating essentially reversible behavior). In the past, surfaces that exhibited reversible behavior were discarded as being too defective without further characterization to confirm surface quality, and cleaved again.[8b,c] Our analysis suggests this is an incorrect interpretation of the voltammetric characteristics. As outlined briefly in Supporting Information, section S1, CV measurements on 20 freshly mechanically cleaved surfaces of HOPG (AM), half of which had capacitance measurements run first, also yielded responses that were close to reversible.

dx.doi.org/10.1021/ja308615h | J. Am. Chem. Soc. 2012, 134, 20117−20130

Figure 2c shows the CV behavior and analysis of a freshly cleaved HOPG electrode (SPI-1 grade) for the reduction of 1 mM $Ru(NH_3)_6^{3+}$ in 1 M aqueous KCl, over the scan rate range 0.01−1 V s^{-1}. The redox process is again close to reversible and the diffusion coefficient for $Ru(NH_3)_6^{3+}$ is calculated as 8.7(±0.3) × 10^{-6} cm^2 s^{-1}, which is in agreement with literature.[40] The data, again, contrasts markedly with previous studies where large ΔE_p has been observed for the $Ru(NH_3)_6^{3+/2+}$ couple, ∼200 mV.[8c,e,i] Reversible behavior has been reported before,[8g] but it was still concluded that the basal surface was totally[9c] or largely inert.[1c,4b]

Time-Dependent Effects. Due to the contrast between the CV behavior seen herein and earlier work, and also in light of microscale and nanoscale measurements reported recently,[1d] we investigated time-dependent effects on the macroscale to ascertain any possible complications associated with voltammetry at HOPG. We first report time effects where CVs were typically recorded at 0.1 V s^{-1} every 5 min in the same solution for up to 2 h. These studies were carried out with commercially available HOPG cleaved by Scotch tape, as this is the cleavage procedure used by researchers in the field in all recent studies[7g,8f,h,24] and many early studies.[8a,b,41] Figure 3 shows data for 1 mM $Fe(CN)_6^{4-}$ (purity 99.99%) in 1 M aqueous KCl on initially freshly cleaved HOPG: (a) ZYA, (b) SPI-1, (c) ZYH, and (d) SPI-2. For all four grades, the ΔE_p value was seen to increase monotonically, with a dramatic change in wave shape and decrease in the magnitude of the current. This behavior is indicative of a systematic diminution in the effective rate of ET as the electrode undergoes repetitive CV. Notably, there is very little difference in the behavior of any of the grades of HOPG even though they have very different step quality (see Table 1). By comparison, for the reduction of 1 mM $Ru(NH_3)_6^{3+}$ in 1 M KCl (0.1 V s^{-1}) at freshly cleaved HOPG (SPI-1 grade), recorded in the same manner, as a function of time, only a small systematic change in the ΔE_p was seen, which ranged between ∼64 mV (first scan) and 77 mV (last scan). The data are given in Supporting Information, section S6. We discuss the origins of these effects and the differences in the two systems in the next sections.

An important consideration for these measurements is the possibility that the composition in the cell changes, due to the finite volume, and that this impacts the subsequent voltammetric response. For a typical sweep rate of 0.1 V s^{-1}, as used above, and in the remaining studies reported herein, the charge passed in the forward wave for $Fe(CN)_6^{4-}$ oxidation was typically 4 × 10^{-6} C, representing ∼0.05% of the total redox-active material in the cell. Furthermore, in the reverse scan most of the electrogenerated $Fe(CN)_6^{3-}$ is converted back to $Fe(CN)_6^{4-}$. Thus, even though a small volume is employed, voltammetry has negligible effect on the bulk solution composition.

Studies at a range of concentrations are valuable as a means of probing surface adsorption and passivation effects. Yet, to our surprise, previous studies of redox processes at HOPG (highlighted in the Introduction) were typically carried out at just one concentration (1 mM). We found that the time-dependent CV response for $Fe(CN)_6^{4-/3-}$ showed a strong concentration effect. Figure 4 shows a plot of ΔE_p against cycle number (5 min between scans) for concentrations of $Fe(CN)_6^{4-/3-}$ between 1 and 10 mM in 1 M KCl. Increasing the concentration of the redox species (and hence flux to the electrode surface) evidently leads to more rapid and more extensive passivation of the electrode surface with a tendency

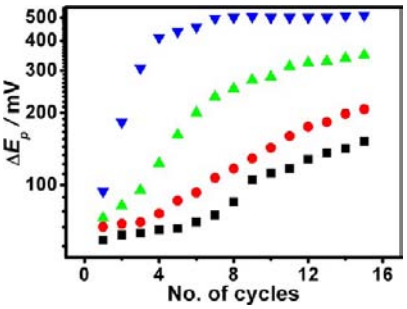

Figure 4. ΔE_p against CV cycle number for concentrations of 1 (■), 2 (●), 5 (▲), and 10 mM (▼) $Fe(CN)_6^{4-}$ in 1 M KCl, run at 0.1 V s^{-1} on SPI-1-grade HOPG.

toward a limiting ΔE_p value of ca. 500 mV on this time scale. The concentration dependence is a clear indication that the observed passivation of the HOPG electrode is due to the electrolysis of the $Fe(CN)_6^{4-/3-}$ couple.

To determine whether the surface passivation could involve just the solution (without voltammetry), experiments were carried out where the solution (1 mM $Fe(CN)_6^{4-}$ (99.99%) in 1 M aqueous KCl), was left for 0 min (black); 1 h (red), and 3 h (green) (at open circuit) on freshly cleaved HOPG before running a CV at 0.1 V s^{-1}. Typical data obtained on SPI-1 HOPG are shown in Figure 5a. It can be seen that the ΔE_p value increases significantly with the time of HOPG surface exposure to solution. This is again evidence of a significant decrease in the effective ET kinetics. Thus, although the oxidation of $Fe(CN)_6^{4-}$ and subsequent reduction of $Fe(CN)_6^{3-}$ "passivates" the HOPG surface, so does simply leaving the $Fe(CN)_6^{4-}$ solution in contact with the surface.

It has been reported that for both HOPG[3c] and a related material, basal plane pyrolytic graphite (BPPG),[4b] simply leaving the surface in air for short periods of time, just a few minutes, resulted in an increase in the ΔE_p value for $Fe(CN)_6^{4-/3-}$. As evident from Figure 5b, we also saw a very similar deterioration in the CV response at HOPG for 1 mM $Fe(CN)_6^{4-}$ in 0.1 M KCl (0.1 V s^{-1}) by comparing immediately after cleaving (black), 1 h wait time before adding the solution (red), and 3 h wait time before adding the solution (green). Interestingly, when the same procedures were carried out for 1 mM $Ru(NH_3)_6^{3+}$ in 0.5 M KCl, no significant change in the ΔE_p value was observed (Figure 5c,d).

Further data for ZYA-grade HOPG, Figure 6, show the effect of cleaving HOPG and leaving the surface in air for 24 h before running CV measurements of (a) 1 mM $Fe(CN)_6^{4-}$ in 0.1 M KCl at 0.1 V s^{-1} and (b) 1 mM $Ru(NH_3)_6^{3+}$ in 0.5 M KCl. Voltammetry for $Fe(CN)_6^{4-/3-}$ is now very irreversible (ΔE_p > 1 V), and for $Ru(NH_3)_6^{3+/2+}$ the behavior is affected ($\Delta E_p \approx$ 115 mV) but much less.

We consider the origin of these various effects in the next section. Importantly, all of these macroscale observations are entirely consistent with our recent SECCM[1d] and SMCM studies.[10c] During SECCM imaging with $Fe(CN)_6^{4-/3-}$, on ZYA HOPG, the response was found to deteriorate during the course of a single scan (duration ∼30 min), immediately after cleaving the HOPG surface, but for $Ru(NH_3)_6^{3+/2+}$ the response was more consistent, with only a small deterioration over time.

The passivation of HOPG by $Fe(CN)_6^{4-/3-}$ voltammetry was found to not only affect the exposed surface but also occasionally the sub-surface, most likely via penetration at step

dx.doi.org/10.1021/ja308615h | J. Am. Chem. Soc. 2012, 134, 20117−20130

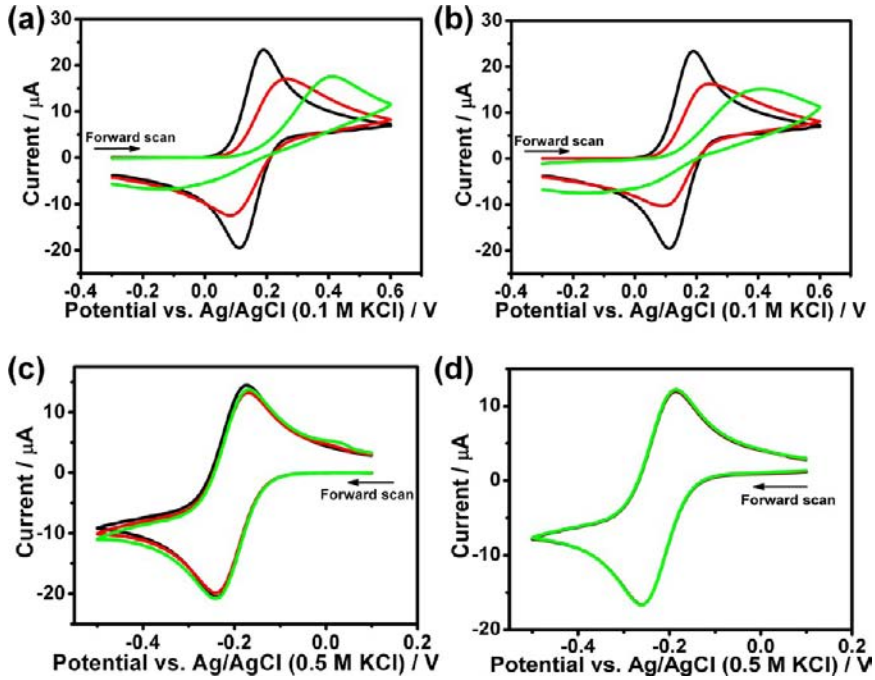

Figure 5. CVs for the oxidation of 1 mM $Fe(CN)_6^{4-}$ in 0.1 M KCl, at 0.1 V s^{-1}: (a) after leaving the solution in contact with the HOPG (SPI-1) for 0 min (black), 1 h (red), and 3 h (green); (b) after a freshly cleaved HOPG (SPI-1) surface was left in air for 0 min (black), 1 h (red), and 3 h (green). CVs for the reduction of 1 mM $Ru(NH_3)_6^{3+}$ in 0.5 M KCl at 0.1 V s^{-1}: (c) after leaving the solution in contact with the HOPG for 0 min (black), 1 h (red), and 3 h (green); (d) after a freshly cleaved HOPG (SPI-1) surface was left in air for 0 min (black), 1 h (red), and 3 h (green). All CVs run on HOPG (SPI-1).

edges, as found for other anions.[42] This is illustrated by Figure 6c, which shows the CV of freshly prepared HOPG (SPI-1 grade) with 1 mM $Fe(CN)_6^{4-}$ in 1 M KCl, after the sample had been fully immersed in solution and cycled extensively, and then cleaved gently once. The CV shows a very irreversible response ($\Delta E_p \approx 1.2$ V).

HOPG Surface Effects. Blocking of the electrode surface would be a plausible reason for the change in ET kinetics for $Fe(CN)_6^{4-/3-}$ with time reported above, and we thus investigated whether such effects occurred via *in situ* TM-AFM experiments. Images of HOPG electrode surfaces (SPI-1 grade) were recorded in solution, before and after the electrode was cycled up to 20 times at 5 min intervals at 0.1 V s^{-1} between 0.0 and 0.6 V, in a solution of 1 mM $Fe(CN)_6^{4-}$ (purity 99.99%) in 1 M KCl. We chose this grade of HOPG because of its use for prominent voltammetric studies,[1c,6a,b,29] and also because the relatively high density of steps (Table 1) allowed us to compare step-edge vs basal regions of the cleaved HOPG surface.

TM-AFM provides simultaneous topographical (height) and phase images. The AFM phase image informs on any changes in energy dissipation during the tip−sample interaction due to changes in topography, tip−sample molecular interactions, and deformation at the tip−sample contact, among other factors.[43] Although difficult to interpret quantitatively, the phase angle is sensitive to changes in the local material properties and can thus provide enhanced contrast. This aspect of TM-AFM is evident in data obtained for HOPG after 1 h in solution (before any voltammetry), where the topography image appears to show a relatively clean surface (Figure 7a-i), while the phase image highlights considerable surface heterogeneity, notably around step edges but also on the basal terrace. This morphological change of the surface links directly to the slower kinetics seen after leaving $Fe(CN)_6^{4-}$ solution in contact with the surface.

After potential cycling, the topography—recorded in the same area as for Figure 7a-i—still appears to indicate a clean surface, but the corresponding phase image evidences further significant local changes in the surface at many locations, which could be indicative of adsorbed material. The images in Figure 7b in fact represent the cleanest surface observed of eight substrates that were potential cycled in separate AFM experiments. For example, Figure 7c shows other behavior, where—after potential cycling—adsorbed material can be seen as discrete topographical features of ca. 5−10 nm in height, which also give rise to significant contrast in the corresponding phase image. Note that during the recording of this image the tip is likely to have picked up material from the surface, as indicated by the sudden change in the phase image part of the way through the scan and the repetition of features in both the topography and phase image ("multiple tip imaging"). Since parts b-ii, c-i, and c-ii of Figure 7 show evidence that material is deposited over the basal surface as well as at the step edges, in agreement with the voltammetric data above, we deduce that blocking of the basal surface of HOPG leads (at least in part) to a diminution in electrode activity for the $Fe(CN)_6^{4-/3-}$ couple.

Additional (control) *in situ* TM-AFM studies were carried out using the same time procedure, but with 1 mM $Ru(NH_3)_6^{3+}$ in 0.5 M KCl, with the HOPG cycled between 0 and −0.8 V, and with just supporting electrolyte (1 M KCl), with the working electrode potential cycled between 0 and 0.6 V. No changes in the topography or in the phase images were seen in either of these cases, even after cycling for up to 2 h. Thus, it is clear that the observed deterioration in electrode kinetics for the $Fe(CN)_6^{4-/3-}$ couple on HOPG is specific to this couple. High resolution imaging and spectroscopic

dx.doi.org/10.1021/ja308615h | J. Am. Chem. Soc. 2012, 134, 20117−20130

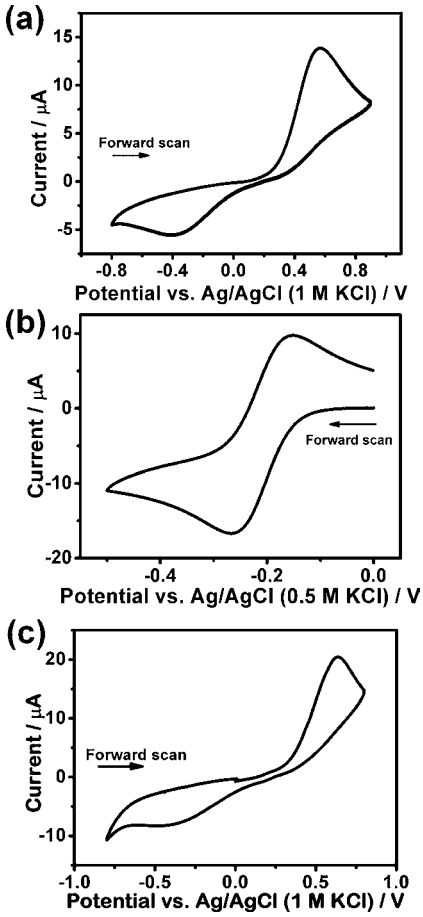

Figure 6. CVs (0.1 V s^{-1}) for (a) the oxidation of 1 mM $Fe(CN)_6^{4-}$ in 1 M KCl and (b) the reduction of 1 mM $Ru(NH_3)_6^{3+}$ in 0.5 M KCl. Each CV was run after the surface of the HOPG (SPI-1) was cleaved and left in air for 24 h. (c) CV for the oxidation of freshly made 1 mM $Fe(CN)_6^{4-}$ in 1 M KCl when the HOPG sample had been in $Fe(CN)_6^{4-}$ solution and cycled between 0 and 0.8 V for over 2 h then gently cleaved once to remove the minimum number of layers but ensuring that the entire surface had been cleaved.

studies[44] for other electrode materials has clearly shown that side products are involved in the $Fe(CN)_6^{3-/4-}$ voltammetric process, leading to the formation of insoluble Prussian Blue-like materials.[44a] It is entirely reasonable to assume that similar processes operate for $Fe(CN)_6^{4-/3-}$ on HOPG.

We have shown for other carbon-based electrodes that maps of the local electroactivity of the surface correspond well to the local intrinsic conductivity of the electrode, as determined by C-AFM.[45] We thus assessed the local conductivity of HOPG, using C-AFM in air, focusing again on SPI-1-grade material, using the protocol outlined in the Experimental Section. Figure 8a,b shows typical (i) height and (ii) conductivity images (5 × 5 μm) recorded simultaneously, at 0.5 Hz, of (a) a freshly cleaved surface and (b) an initially freshly cleaved surface that was left in air for 24 h before imaging. Note that slight "streaking" seen, also evident in previous C-AFM images of HOPG,[46] is likely due to variations in the tip to surface contact, as the tip scans the surface, but does not impact the capability to identify the general surface conductivity properties of HOPG.

It is evident that although the surface is conducting, the current varies from terrace to terrace. To provide further information on the local conductivity of the HOPG surface, C-

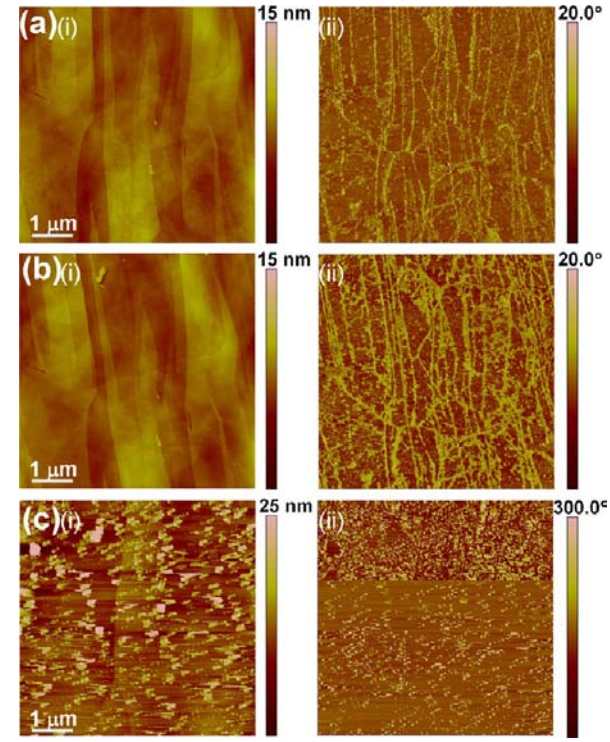

Figure 7. *In situ* TM-AFM height (i) and phase (ii) images taken on HOPG (SPI-1) during CV measurements run at 0.1 V s^{-1} in 1 mM $Fe(CN)_6^{4-}$ (purity 99.99%) in 1 M aqueous KCl: (a) before the first CV was run; (b) in the same area as (a) after 20 cycles; and (c) a different sample after 20 cycles were run.

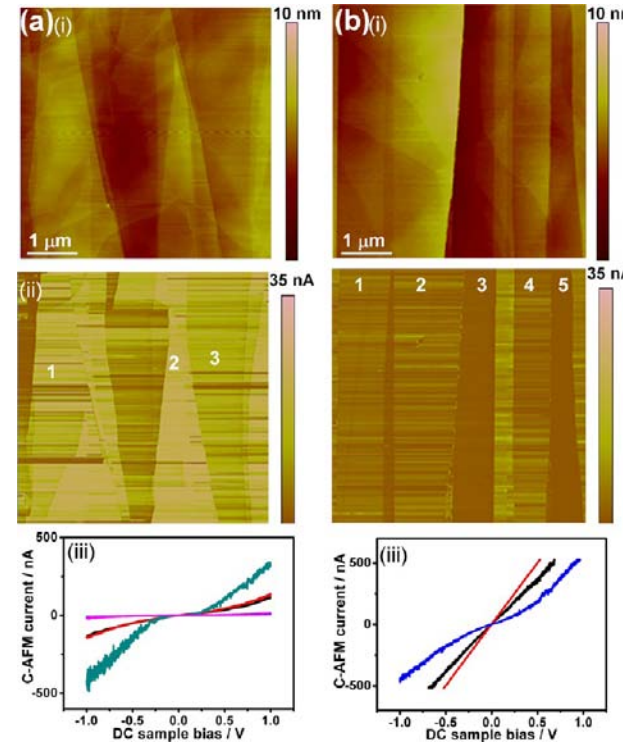

Figure 8. Simultaneously recorded height (i) and conductivity (ii) images (5 × 5 μm) on HOPG (SPI-1) immediately after cleavage (a) and 24 h after cleavage (b). (iii) C-AFM *i*–*V* curves recorded in terrace locations 1, 2, and 3 marked on panel a-ii and terrace locations 1, 2, 3, 4, and 5 marked on panel b-ii.

dx.doi.org/10.1021/ja308615h | *J. Am. Chem. Soc.* 2012, 134, 20117–20130

AFM ($i-V$) curves were recorded in distinct regions of the basal surface, which showed different current levels in the C-AFM map. Three such curves are shown in Figure 8a-iii, recorded in the vicinity of the terrace regions labeled 1 (black), 2 (red), and 3 (blue) in Figure 8a-ii. In all cases the $i-V$ curves recorded repeatedly in the same spot overlapped (n = 5). For these three different characteristic $i-V$ curves, local resistance (R) values were extracted in the low bias region i.e. −100 mV to +100 mV yielding R = 1.3 MΩ (terrace 1), R = 1 MΩ (terrace 2), and R = 3.7 MΩ (terrace 3). Note that these values include the 1 MΩ resistor placed in series in the experimental measurements to limit the current flowing and possible damage to the metal-coated tip.

Figure 8b shows that the conductivity of the surface, after 24 h exposure to the atmosphere, is dramatically altered compared to the freshly cleaved case (Figure 8a), with some domains essentially inert at the applied potential bias and others showing greatly reduced conductivity. By recording $i-V$ curves in the vicinity of the five different terraces labeled in Figure 8b-iii, R values were extracted in the region of low bias: R = 13 MΩ (terrace 1), R = 13 MΩ (terrace 2), R = 268 MΩ (terrace 3), R = 26 MΩ (terrace 4), and R = 267 MΩ (terrace 5), with a 1 MΩ resistor in series. These raw values are 1−2 orders of magnitude higher than the R values recorded on the freshly cleaved surface, and indicate a change in either tip−surface contact resistance or the local resistance of the HOPG surface layers of at least 3 orders of magnitude in some locations (taking into account the current-limiting resistor). The $i-V$ curves all show a non-linear increase in the current at high bias.

The C-AFM data clearly show that long time exposure of HOPG to ambient conditions results in a significant increase in the local resistance of the surface compared to a freshly cleaved surface. In fact the deterioration in basal plane conductivity occurs on a fairly rapid time scale as shown in Supporting Information, section S7. It has been reported[8g] that polished and cleaved BPPG exposed to air for up to 2 h, resulted in increasing kinetic effects for $Fe(CN)_6^{4-/3-}$. This was attributed purely to the oxygenation of edge planes. Although we cannot rule this out or in, our data clearly indicate that gross changes in the conductivity of much of the exposed basal surface are most important in the case of HOPG (and, by extension, to BPPG as well). It is well known that HOPG voltammetry is notoriously sensitive to deliberate treatment of the surface with organic impurities.[47] Naturally, extended periods, under ambient conditions, enhances the chance of the surface becoming contaminated, which would result in a greater contact resistance and tunneling barrier between the C-AFM tip and the HOPG surface. Such a barrier layer would naturally also influence voltammetric behavior, and links convincingly to the electrochemical studies presented above. It is also possible that the top layer(s) of the HOPG could spontaneously delaminate leading to poor electrical contact. Evidently, the C-AFM studies highlight new issues connected with HOPG surface properties which may impact the analysis of earlier work,[1a,8e−g,9a,c,15,41] and need to be taken into account in the design and analysis of future studies of HOPG and graphene.

Nanoscale Visualization of Electrochemical Activity with SECCM. SECCM is a powerful imaging technique for the simultaneous study of topography, surface electroactivity and conductivity, where the meniscus at the end of a pipet is used as a positionable and moveable nanoelectrochemical cell once contacted with a electrode surface (Figure 9).[1d,14m,30,48] The pipet tip was oscillated perpendicular to the substrate, giving

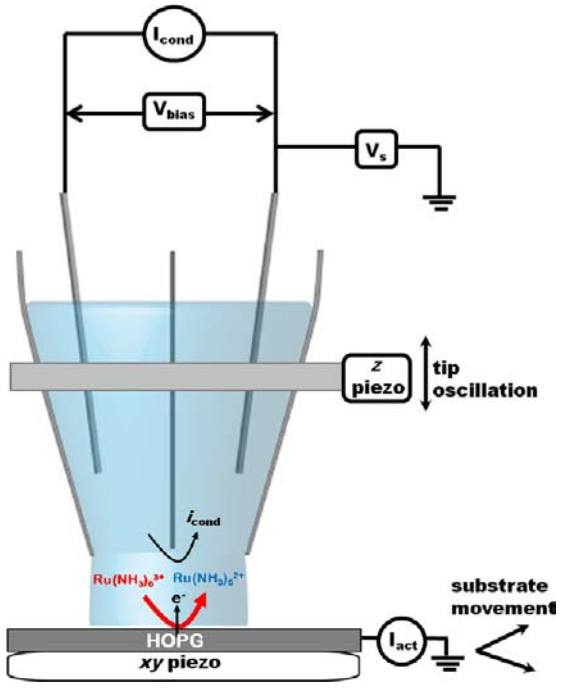

Figure 9. Schematic of the setup for SECCM (see text for description).

rise to a modulated current, I_{AC}, and increase in the DC conductance current when the meniscus made contact with the surface. As described in the Experimental Section, and in full elsewhere,[30] I_{AC} is used as a set-point for imaging during which the surface electrochemical current, I_{act}, at an effective bias of $-(V_s + 1/2\ V_{bias})$, with respect to the QRCEs in the pipet, is recorded. This technique has recently been used to visualize electrochemistry at cleaved ZYA-grade HOPG[1d] where the spatial contact was an order of magnitude smaller than the step spacing. This study showed conclusively that essentially uniform and fast electrochemical activity prevailed for the reduction of $Ru(NH_3)_6^{3+}$ at the basal surface of HOPG. As highlighted above (Figure 1 and Table 1), the step spacing on mechanically cleaved HOPG (AM) is even larger than on Scotch tape cleaved ZYA-grade HOPG, and as HOPG (AM) has been proposed as the key material and mechanical cleavage the optimal procedure[1c] we considered it worthwhile to map its local electrochemical activity. As there are major complications involved in using the $Fe(CN)_6^{4-/3-}$ couple, as evidenced in our previous imaging studies[1d,10c] and the macroscopic measurements reported herein, we chose to focus on the $Ru(NH_3)_6^{3+/2+}$ couple.

Figure 10 shows SECCM maps of (a) quasi-topography, (b) surface electrochemical activity, and (c) conductance current recorded between the barrels of the SECCM tip obtained for the reduction of 1 mM $Ru(NH_3)_6^{3+}$ in 0.1 M KCl at a potential close to the reversible quarter-wave potential, as determined by SECCM voltammetry, on mechanically cleaved HOPG (AM). Parallel steps running across the surface with a basal region spanning up to 5 μm in length is clearly evident at the right-hand side of the maps of quasi-topography (a) and SECCM conductance (c). Importantly, the surface activity (b) can be seen to be essentially constant at approximately 12.7 ± 1.0 pA (1σ). For this tip, the mass transport limited current was ca. 60 pA, and so the surface redox process measured is close to reversible across the basal surface of HOPG (AM). Based on

dx.doi.org/10.1021/ja308615h | J. Am. Chem. Soc. 2012, 134, 20117−20130

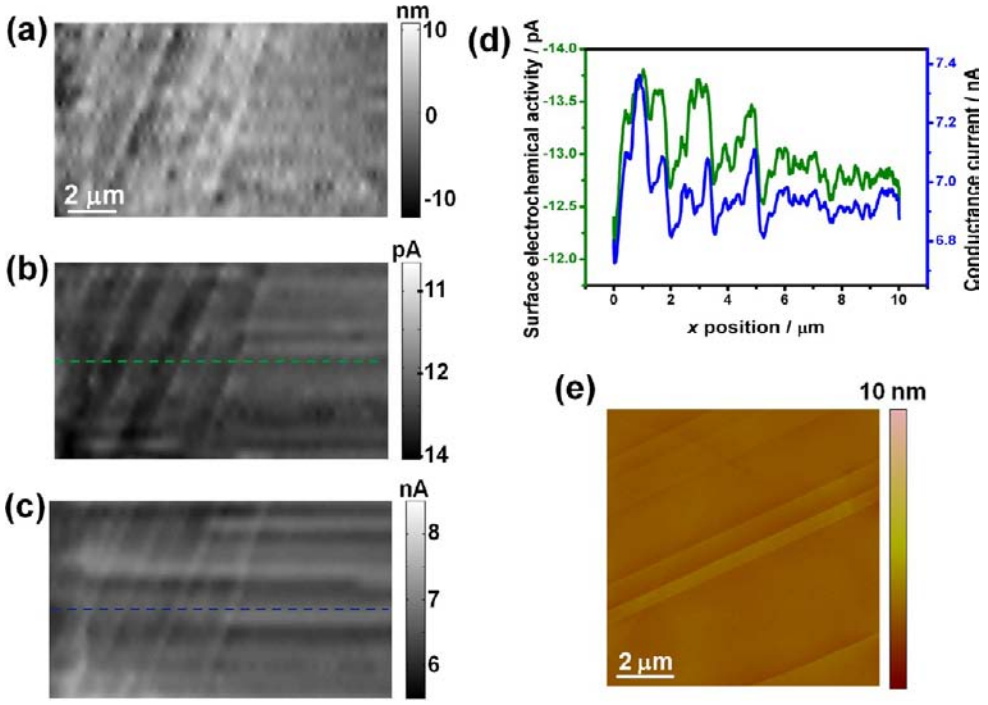

Figure 10. SECCM maps of (a) quasi-topography, (b) surface electrochemical activity, and (c) conductance current (DC component) recorded at the reversible quarter-wave potential for the reduction of 1 mM $Ru(NH_3)_6^{3+}$ at HOPG (AM) mechanically cleaved obtained with a ~350 nm pipet. (d) Example line section of surface electrochemical activity (green) and conductance current (blue) from marked regions in (b) and (c). (e) AFM image representative of the surface.

the arguments advanced recently,[1d] we estimate a mass transfer coefficient ca. 0.25 cm s^{-1}, on the basis of meniscus contact area approximating to the tip opening and the limiting current defined above, from which we put a lower limit ca. 0.1 cm s^{-1} on the standard rate constant for the $Ru(NH_3)_6^{3+/2+}$ couple.

As in our recent study of ZYA-grade HOPG,[1d] a small increase in surface electrochemical current (Figure 10b) is observed at the step sites, but there is also an increase in the conductance current between the barrels of the SECCM tip at the same locations (Figure 10c), likely due to a small disturbance in the meniscus as it passes over (hydrophilic) step edges.[1d] This effect is shown very clearly in the line scans of surface electrochemical current and corresponding conductance current in Figure 10d. A representative AFM image of mechanically cleaved HOPG (AM) in an area close to the SECCM measurements, recorded after the SECCM measurements, shows that there are step separations greater than 5 μm in this region of the surface (Figure 10e), consistent with the SECCM measurements. Thus, the nanoscopic SECCM visualization studies on pristine, freshly cleaved HOPG show that heterogeneous ET occurs readily at the basal surface, entirely consistent with the macroscopic measurements, but providing a clear view as to the origin of the electroactivity.

CONCLUDING REMARKS

We have reappraised classical voltammetry at the basal surface of HOPG, a material of intrinsic importance, but also one that is gaining increasing prominence as a "standard" to which new sp^2 carbon materials, such as CNTs and graphene, are compared. Making extensive use of high resolution microscopy to understand the surface characteristics of HOPG, the studies reported herein provide a new and self-consistent view of the electroactivity, tying together macroscale, microscale and nanoscale measurements. Our results show unequivocally that the pristine HOPG surface, which has been variously described as supporting only sluggish ET behavior,[8a−e,20−22,35,41,49] or even as being completely inert,[8f,g,9,17,24,50] has, in fact, considerable ET activity.

The freshly cleaved basal surfaces of five different grades of HOPG, cleaved by Scotch tape or a mechanical procedure, show essentially reversible voltammetry for both $Fe(CN)_6^{4-/3-}$ and $Ru(NH_3)_6^{3+/2+}$ on the CV time scale. The general quality and step-edge density of these surfaces has been fully characterized by AFM. For ZYA and SPI-1 material cleaved by Scotch tape and HOPG (AM) cleaved mechanically, the quality of the surfaces has been further confirmed by capacitance measurements, as recommended in the early literature.[8b,c,e] These HOPG samples provide a range of step-edge densities on the basal surface and, in the context of ZYA grade and AM material, particularly low step-edge densities (among the lowest reported) and a basal surface of high quality. This range of surfaces has enabled the significance of steps edges, in the HOPG electrode response, to be explored and identified. The analysis of this wide range of materials is further important in light of a recent report[51] of the inclusion of micrometer-sized Fe-containing particles in ZY materials, albeit with rather large (100−200 μm) lateral spacing, which is unlikely to impact macroscale electrochemistry. In contrast, SPI materials do not show such inclusions.[51]

Significantly, the new view of the macroscopic electrochemical response agrees entirely with recent direct microscale and nanoscale studies of basal surface HOPG,[1d,10] and further SECCM studies reported herein. It is important to note that the basal surface itself will contain point (atom-scale) defects, which may have a higher local density of electronic states.[52] Such sites could have different local ET activity, compared to the basal terrace surface or indeed control the activity of the

dx.doi.org/10.1021/ja308615h | J. Am. Chem. Soc. 2012, 134, 20117−20130

basal terrace, but this has not, hitherto, been considered an issue needed to explain the voltammetric response of HOPG. Determining the significance, if any, of such sites would require the preparation and characterization of HOPG materials with different densities of point defects, which is nontrivial,[51] and/or further improvement of nanoscale electrochemical imaging methods, which could eventually have sufficiently high resolution to address this issue directly.[30,48c,53]

Our CV measurements on freshly cleaved surfaces conflict with many other high-profile studies in the literature,[5a,6a−e,8] which are frequently cited as evidence that the basal surfaces of sp^2 carbon materials are essentially inert in terms of ET.[1g,8,17,49a] Extensive studies reported in this paper, exploring HOPG surface and time effects were aimed at rationalizing and explaining our data in the context of this past work. A significant finding is that $Fe(CN)_6^{4-}$ solution and voltammetry leads to the surface-adsorption of material which greatly impedes subsequent ET for the $Fe(CN)_6^{4-/3-}$ couple. Likewise, after cleaving, there are major time-dependent changes in the surface conductance properties of HOPG, probably by adsorbed impurities and/or other changes in the HOPG surface layer, which correlates with a measured deterioration in the $Fe(CN)_6^{4-/3-}$ voltammetric response.

On the other hand, the surface effects observed (blocking of the HOPG electrode and changes in the surface conductivity) have much less influence on $Ru(NH_3)_6^{3+/2+}$ voltammetry at the macroscale. Of course, time-dependent changes in surface activity may occur on the microscale and nanoscale and we plan to investigate the significance, if any, of such effects for $Ru(NH_3)_6^{3+/2+}$ in the future. In light of the work herein, it is unfortunate that $Fe(CN)_6^{4-/3-}$ voltammetry was selected as a means for "surface validation" [8a−e] of HOPG for the subsequent study of further redox couples whose ET kinetics may have been impaired, and that it has been used extensively as a redox probe to assess ET activity at the basal surface of HOPG.[1g,8f,g,9b,c,50a]

The surface effects we have observed occur on a short time scale and become more prevalent over longer time scales (typically a few CVs, or a time scale of an hour or more). In some instances, the CV morphologies that result are then similar to some of those in the past literature. For example, the CVs for $Fe(CN)_6^{4-/3-}$ after extensive cycling (Figure 3) and after deploying a wait time of a few hours before cycling (Figure 5a,c) resemble those in refs 8g and 9c. Similarly, the very distorted voltammograms evident after leaving HOPG for a long period before running voltammetry (Figure 6a) and cleaving after extensively cycling (Figure 6c) resemble the morphology of those reported previously.[1g,8a,e,f,h,i,17] Some of these past studies provide little information on the precise time frame of the measurements, although they evidently aim to consider pristine surfaces.[1g,8f,h,i,17] The results herein thus potentially provide an explanation of this past work, particularly as we have worked with identical HOPG material from the same supplier, and cleaved in the same way. On the other hand, in the oldest body of past work measurements were made immediately after cleaving HOPG.[8b,c] In view of this, it is difficult to explain the difference in initial CV behavior seen in our work and these past studies, but if impurity adsorption (and other surface effects) were responsible for the dramatic deterioration we have observed in HOPG surface conductivity, and concomitant changes in the $Fe(CN)_6^{4-/3-}$ voltammetric response, one might reasonably expect different time scales for such processes in different laboratories/environments and, of course, in different eras. Alternative explanations for the discrepancy between the work of McCreery et al. and the current work include possible differences in the HOPG samples or that the "validation" method for identifying low defect surfaces was erroneous.

It is important to point out that the reversible (or fast ET) we report herein for $Fe(CN)_6^{4-/3-}$ on freshly cleaved HOPG has been seen by others for HOPG.[6c,47,49b] However, in light of the earlier recommendations about the $Fe(CN)_6^{4-/3-}$ couple being diagnostic of surface quality,[8a−e,35] it was assumed that in those studies[6c,47,49b] the HOPG surfaces used must have been very defective, although no other corroboratory evidence was provided. Our studies clearly establish that the pristine basal surface of a wide range of HOPG (AM, ZYA, ZYH, SPI-1, and SPI-2) provides an active electrode material for ET, as evident from studies of both $Fe(CN)_6^{4-/3-}$ and $Ru(NH_3)_6^{3+/2+}$. Finally, this new view of the electroactivity of the HOPG basal surface, and the important issues concerning the use of $Fe(CN)_6^{4-/3-}$ and the time scale of measurements, are expected to be valuable for rationalizing different viewpoints on other sp^2 carbon materials. In particular, $Fe(CN)_6^{4-/3-}$ has been used in recent studies of the electrochemical properties of monolayer and multilayer graphene,[1a,15b,25] and comparisons have generally been made between graphene and HOPG.[15b,25] It is evident from our studies that $Fe(CN)_6^{4-/3-}$ should be used with caution for such studies in the future, if at all. Moreover, electrochemical studies of exfoliated graphene, in particular, need careful control and identification of the measurement time after exfoliation.

■ ASSOCIATED CONTENT

Supporting Information

Additional details on capacitance measurements, experimental procedures, step-edge analysis using AFM, and FE-SEM and C-AFM experiments. This material is available free of charge via the Internet at http://pubs.acs.org.

■ AUTHOR INFORMATION

Corresponding Author

p.r.unwin@warwick.ac.uk

Present Address

[+]Laboratoire Pasteur, Département de Chimie, Ecole Normale Supérieure, CNRS, UPMC Univ Paris 06, 24 Rue Lhomond, Paris, France

Notes

The authors declare no competing financial interest.

■ ACKNOWLEDGMENTS

We thank the EPSRC (grant numbers EP/H023909/1 and EP/F064861/1) and the European Research Council (grant number ERC-2009-AdG 247143-QUANTIF) for support. M.G.C. was supported by a Marie Curie Intra-European Fellowship. We are grateful to Syngenta and the EPSRC for funding for M.A.O'C and to the EPSRC for supporting K.M. by funding of the MOAC Doctoral Training Centre. We thank Dr. Neil Wilson and Mr. Steve York for assistance with AFM measurements and FE-SEM imaging, respectively, and Dr. Silvia Rabar and Dr. Sara Dale for preliminary measurements. We are grateful to Dr. Dallal Stevens, Prof. Mark Newton, and Dr. Stanley Lai at the University of Warwick for generous advice and suggestions during the course of this work. Some of the equipment used in this work was obtained through the

Science City Advanced Materials project with support from Advantage West Midlands and the European Regional Development Fund. We thank Prof. R. L. McCreery (University of Alberta, Canada) for providing the sample of HOPG used for some of the studies reported herein.

REFERENCES

(1) (a) Rodriguez-Lopez, J.; Ritzert, N. L.; Mann, J. A.; Tan, C.; Dichtel, W. R.; Abruna, H. D. *J. Am. Chem. Soc.* **2012**, *134*, 6224−6236. (b) Ward, K. R.; Lawrence, N. S.; Hartshorne, R. S.; Compton, R. G. *Phys. Chem. Chem. Phys.* **2012**, *14*, 7264−7275. (c) McCreery, R. L.; McDermott, M. T. *Anal. Chem.* **2012**, *84*, 2602−2605. (d) Lai, S. C. S.; Patel, A. N.; McKelvey, K.; Unwin, P. R. *Angew. Chem., Int. Ed.* **2012**, *51*, 5405−5408. (e) Dumitrescu, I.; Unwin, P. R.; Macpherson, J. V. *Chem. Commun.* **2009**, *7345*, 6886−6901. (f) McCreery, R. L. *Chem. Rev* **2008**, *108*, 2646−2687. (g) Banks, C. E.; Davies, T. J.; Wildgoose, G. G.; Compton, R. G. *Chem. Commun.* **2005**, 829−841. (h) Pumera, M. *Chem. Soc. Rev.* **2010**, *39*, 4146−4157.

(2) (a) Alwarappan, S.; Erdem, A.; Liu, C.; Li, C.-Z. *J. Phys. Chem. C* **2009**, *113*, 8853−8857. (b) Chen, F.; Qing, Q.; Xia, J.; Li, J.; Tao, N. *J. Am. Chem. Soc.* **2009**, *131*, 9908−9909. (c) Shan, C.; Yang, H.; Song, J.; Han, D.; Ivaska, A.; Niu, L. *Anal. Chem.* **2009**, *81*, 2378−2382. (d) Tang, L.; Wang, Y.; Li, Y.; Feng, H.; Lu, J.; Li, J. *Adv. Funct. Mater.* **2009**, *19*, 2782−2789. (e) Wang, Y.; Shi, Z.; Huang, Y.; Ma, Y.; Wang, C.; Chen, M.; Chen, Y. *J. Phys. Chem. C* **2009**, *113*, 13103−13107. (f) Zhou, M.; Zhai, Y.; Dong, S. *Anal. Chem.* **2009**, *81*, 5603−5613.

(3) (a) Jouikov, V.; Simonet, J. *Langmuir* **2012**, *28*, 931−938. (b) Bhattacharjya, D.; Mukhopadhyay, I. *Langmuir* **2012**, *28*, 5893−5899. (c) Mas-Torrent, M.; Crivillers, N.; Rovira, C.; Veciana, J. *Chem Rev* **2012**, *112*, 2506−2527. (d) Hui, F.; Noel, J. M.; Poizot, P.; Hapiot, P.; Simonet, J. *Langmuir* **2011**, *27*, 5119−5125.

(4) (a) Crevillen, A. G.; Pumera, M.; Gonzalez, M. C.; Escarpa, A. *Analyst* **2009**, *134*, 657−662. (b) Banks, C. E.; Crossley, A.; Salter, C.; Wilkins, S. J.; Compton, R. G. *Angew. Chem., Int. Ed.* **2006**, *45*, 2533−2537.

(5) (a) Liu, H.; Favier, F.; Ng, K.; Zach, M. P.; Penner, R. M. *Electrochim. Acta* **2001**, *47*, 671−677. (b) Menke, E. J.; Li, Q.; Penner, R. M. *Nano Lett.* **2004**, *4*, 2009−2014. (c) Penner, R. M. *J. Phys. Chem. B* **2002**, *106*, 3339−3353. (d) Zoval, J. V.; Stiger, R. M.; Biernacki, P. R.; Penner, R. M. *J. Phys. Chem.* **1996**, *100*, 837−844. (e) Boxley, C. J.; White, H. S.; Lister, T. E.; Pinhero, P. J. *J. Phys. Chem. B* **2003**, *107*, 451−458. (f) Gloaguen, F.; Leger, J. M.; Lamy, C.; Marmann, A.; Stimming, U.; Vogel, R. *Electrochim. Acta* **1999**, *44*, 1805−1816. (g) Zubimendi, J. L.; Vazquez, L.; Ocon, P.; Vara, J. M.; Triaca, W. E.; Salvarezza, R. C.; Arvia, A. J. *J. Phys. Chem.* **1993**, *97*, 5095−5102. (h) Hendricks, S. A.; Kim, Y.-T.; Bard, A. J. *J. Electrochem. Soc.* **1992**, *139*, 2818−2824.

(6) (a) González Orive, A.; Grumelli, D.; Vericat, C.; Ramallo-López, J. M.; Giovanetti, L.; Benitez, G.; Azcárate, J. C.; Corthey, G.; Fonticelli, M. H.; Requejo, F. G.; Hernández Creus, A.; Salvarezza, R. C. *Nanoscale* **2011**, *3*, 1708−1716. (b) Brülle, T.; Stimming, U. *J. Electroanal. Chem.* **2009**, *636*, 10−17. (c) Peruffo, M.; Contreras-Carballada, P.; Bertoncello, P.; Williams, R. M.; Cola, L. D.; Unwin, P. R. *Electrochem. Commun.* **2009**, *11*, 1885−1887. (d) Rodríguez-Nieto, F. J.; Morante-Catacora, T. Y.; Cabrera, C. R. *J. Electroanal. Chem.* **2004**, *571*, 15−26. (e) Cherstiouk, O. V.; Simonov, P. A.; Savinova, E. R. *Electrochim. Acta* **2003**, *48*, 3851−3860. (f) Surendranath, Y.; Lutterman, D. A.; Liu, Y.; Nocera, D. G. *J. Am. Chem. Soc.* **2012**, *134*, 6326−6336.

(7) (a) Zach, M. P.; Inazu, K.; Ng, K. H.; Hemminger, J. C.; Penner, R. M. *Chem. Mater.* **2002**, *14*, 3206−3216. (b) Armstrong, F. A.; Bond, A. M.; Hill, H. A. O.; Oliver, B. N.; Psalti, I. S. M. *J. Am. Chem. Soc.* **1989**, *111*, 9185−9189. (c) Armstrong, F. A.; Bond, A. M.; Hill, H. A. O.; Psalti, I. S. M.; Zoski, C. G. *J. Phys. Chem.* **1989**, *93*, 6485−6493. (d) Gorodetsky, A. A.; Barton, J. K. *J. Am. Chem. Soc.* **2007**, *129*, 6074−6075. (e) Gorodetsky, A. A.; Barton, J. K. *Langmuir* **2006**, *22*, 7917−7922. (f) Hui, F.; Noël, J.-M.; Poizot, P.; Hapiot, P.; Simonet, J. *Langmuir* **2011**, *27*, 5119−5125. (g) Bradbury, C. R.; Kuster, L.; Fermín, D. J. *J. Electroanal. Chem.* **2010**, *646*, 114−123. (h) Wang, M.; Bugarski, S.; Stimming, U. *J. Phys. Chem. C* **2008**, *112*, 5165−5173. (i) Ventosa, E.; Palacios, J. L.; Unwin, P. R. *Electrochem. Commun.* **2008**, *10*, 1752−1755.

(8) (a) Bowling, R. J.; Packard, R. T.; McCreery, R. L. *J. Am. Chem. Soc.* **1989**, *111*, 1217−1223. (b) Rice, R. J.; McCreery, R. L. *Anal. Chem.* **1989**, *61*, 1637−1641. (c) Kneten, K. R.; McCreery, R. L. *Anal. Chem.* **1992**, *64*, 2518−2524. (d) McDermott, M. T.; Kneten, K.; McCreery, R. L. *J. Phys. Chem.* **1992**, *96*, 3124−3130. (e) Cline, K. K.; Mcdermott, M. T.; McCreery, R. L. *J. Phys. Chem.* **1994**, *98*, 5314−5319. (f) Davies, T. J.; Moore, R. R.; Banks, C. E.; Compton, R. G. *J. Electroanal. Chem.* **2004**, *574*, 123−152. (g) Ji, X.; Banks, C. E.; Crossley, A.; Compton, R. G. *ChemPhysChem* **2006**, *7*, 1337−1344. (h) Lee, C.-Y.; Guo, S.-X.; Bond, A. M.; Oldham, K. B. *J. Electroanal. Chem.* **2008**, *615*, 1−11. (i) Lee, C.-Y.; Bond, A. M. *Anal. Chem.* **2009**, *81*, 584−594.

(9) (a) Moore, R. R.; Banks, C. E.; Compton, R. G. *Analyst* **2004**, *129*, 755−758. (b) Banks, C. E.; Moore, R. R.; Davies, T. J.; Compton, R. G. *Chem. Commun.* **2004**, 1804−1805. (c) Davies, T. J.; Hyde, M. E.; Compton, R. G. *Angew. Chem.* **2005**, *44*, 5121−5126. (d) Hyde, M. E.; Davies, T. J.; Compton, R. G. *Angew. Chem., Int. Ed.* **2005**, *44*, 6491−6496. (e) Ji, X. B.; Buzzeo, M. C.; Banks, C. E.; Compton, R. G. *Electroanalysis* **2006**, *18*, 44−52.

(10) (a) Edwards, M. A.; Bertoncello, P.; Unwin, P. R. *J. Phys. Chem. C* **2009**, *113*, 9218−9223. (b) Frederix, P. L.; Bosshart, P. D.; Akiyama, T.; Chami, M.; Gullo, M. R.; Blackstock, J. J.; Dooleweerdt, K.; de Rooij, N. F.; Staufer, U.; Engel, A. *Nanotechnology* **2008**, *19*, 384004. (c) Williams, C. G.; Edwards, M. A.; Colley, A. L.; Macpherson, J. V.; Unwin, P. R. *Anal. Chem.* **2009**, *81*, 2486−2495. (d) Anne, A.; Cambril, E.; Chovin, A.; Demaille, C.; Goyer, C. *ACS Nano* **2009**, *3*, 2927−2940.

(11) Yang, W.; Ratinac, K. R.; Ringer, S. P.; Thordarson, P.; Gooding, J. J.; Braet, F. *Angew. Chem., Int. Ed.* **2010**, *49*, 2114−2138.

(12) Banks, C. E.; Hallam, P. M. *Electrochem. Commun.* **2011**, *13*, 8−11.

(13) (a) Chou, A.; Bocking, T.; Singh, N. K.; Gooding, J. J. *Chem. Commun.* **2005**, 842−844. (b) Gong, K.; Chakrabarti, S.; Dai, L. *Angew. Chem., Int. Ed.* **2008**, *47*, 5446−5450.

(14) (a) Bertoncello, P.; Edgeworth, J. P.; Macpherson, J. V.; Unwin, P. R. *J. Am. Chem. Soc.* **2007**, *129*, 10982−10983. (b) Day, T. M.; Unwin, P. R.; Macpherson, J. V. *Nano Lett.* **2007**, *7*, 51−57. (c) Day, T. M.; Unwin, P. R.; Wilson, N. R.; Macpherson, J. V. *J. Am. Chem. Soc.* **2005**, *127*, 10639−10647. (d) Dudin, P. V.; Unwin, P. R.; Macpherson, J. V. *J. Phys. Chem. C* **2010**, *114*, 13241−13248. (e) Dumitrescu, I.; Dudin, P. V.; Edgeworth, J. P.; Macpherson, J. V.; Unwin, P. R. *J. Phys. Chem. C* **2010**, *114*, 2633−2639. (f) Dumitrescu, I.; Unwin, P. R.; Wilson, N. R.; Macpherson, J. V. *Anal. Chem.* **2008**, *80*, 3598−3605. (g) Snowden, M. E.; Unwin, P. R.; Macpherson, J. V. *Electrochem. Commun.* **2011**, *13*, 186−189. (h) Wilson, N. R.; Guille, M.; Dumitrescu, I.; Fernandez, V. R.; Rudd, N. C.; Williams, C. G.; Unwin, P. R.; Macpherson, J. V. *Anal. Chem.* **2006**, *78*, 7006−7015. (i) Heller, I.; Kong, J.; Heering, H. A.; Williams, K. A.; Lemay, S. G.; Dekker, C. *Nano Lett.* **2005**, *5*, 137−142. (j) Heller, I.; Kong, J.; Williams, K. A.; Dekker, C.; Lemay, S. G. *J. Am. Chem. Soc.* **2006**, *128*, 7353−7359. (k) Kim, J.; Xiong, H.; Hofmann, M.; Kong, J.; Amemiya, S. *Anal. Chem.* **2010**, *82*, 1605−1607. (l) Miller, T. S.; Ebejer, N.; Guëll, A. G.; Macpherson, J. V.; Unwin, P. R. *Chem Commun (Camb)* **2012**, *48*, 7435−7437. (m) Guëll, A. G.; Ebejer, N.; Snowden, M. E.; McKelvey, K.; Macpherson, J. V.; Unwin, P. R. *Proc. Natl. Acad. Sci. U.S.A.* **2012**, *109*, 11487−11492.

(15) (a) Li, W.; Tan, C.; Lowe, M. A.; Abruña, H. D.; Ralph, D. C. *ACS Nano* **2011**, *5*, 2264−2270. (b) Valota, A. T.; Kinloch, I. A.; Novoselov, K. S.; Casiraghi, C.; Eckmann, A.; Hill, E. W.; Dryfe, R. A. W. *ACS Nano* **2011**, *5*, 8809−8815.

(16) Heller, I.; Janssens, A. M.; Männik, J.; Minot, E. D.; Lemay, S. G.; Dekker, C. *Nano Lett.* **2008**, *8*, 591−595.

(17) Banks, C. E.; Compton, R. G. *The Analyst* **2006**, *131*, 15−21.

(18) Amatore, C.; Savéant, J. M.; Tessier, D. *J. Electroanal. Chem.* **1983**, *147*, 39−51.

(19) Chang, H.; Bard, A. J. *Langmuir* **1991**, *7*, 1143−1153.
(20) McDermott, M. T.; McCreery, R. L. *Langmuir* **1994**, *10*, 4307−4314.
(21) Robinson, R. S.; Sternitzke, K.; Mcdermott, M. T.; McCreery, R. L. *J. Electrochem. Soc.* **1991**, *138*, 2412−2418.
(22) Ray, K.; McCreery, R. L. *Anal. Chem.* **1997**, *69*, 4680−4687.
(23) Macpherson, J. V.; Unwin, P. R. *Anal. Chem.* **2000**, *72*, 276−285.
(24) Bowler, R.; Davies, T. J.; Hyde, M. E.; Compton, R. G. *Anal. Chem.* **2005**, *77*, 1916−1919.
(25) Tan, C.; Rodriguez-Lopez, J.; Parks, J. J.; Ritzert, N. L.; Ralph, D. C.; Abruna, H. D. *ACS Nano* **2012**, *6*, 3070−3079.
(26) Hassel, A. W.; Fushimi, K.; Seo, M. *Electrochem. Commun.* **1999**, *1*, 180−183.
(27) Gewirth, A. A.; Bard, A. J. *J. Phys. Chem.* **1988**, *92*, 5563−5566.
(28) Hathcock, K. W.; Brumfield, J. C.; Goss, C. A.; Irene, E. A.; Murray, R. W. *Anal. Chem.* **1995**, *67*, 2201−2206.
(29) Unwin, P. R.; Bard, A. J. *Anal. Chem.* **1992**, *64*, 113−119.
(30) Snowden, M. E.; Guëll, A. G.; Lai, S. C.; McKelvey, K.; Ebejer, N.; O'Connell, M. A.; Colburn, A. W.; Unwin, P. R. *Anal. Chem.* **2012**, *84*, 2483−2491.
(31) Rodolfa, K. T.; Bruckbauer, A.; Zhou, D.; Korchev, Y. E.; Klenerman, D. *Angew. Chem., Int. Ed.* **2005**, *44*, 6854−6859.
(32) Laslau, C.; Williams, D. E.; Travas-Sejdic, J. *Prog. Polym. Sci.* **2012**, *37*, 1177−1191.
(33) Xu, J.; Chen, Q.; Swain, G. M. *Anal. Chem.* **1998**, *70*, 3146−3154.
(34) (a) Jandt, K. *Surf. Sci.* **2001**, *491*, 303−332. (b) Carswell, A. D. W.; O'Rear, E. A.; Grady, B. P. *J. Am. Chem. Soc.* **2003**, *125*, 14793−14800. (c) Ta, T. C.; Sykes, M. T.; McDermott, M. T. *Langmuir* **1998**, *14*, 2435−2443.
(35) McCreery, R. L.; Cline, K. K.; McDermott, C. A.; McDermott, M. T. *Colloids Surf., A* **1994**, *93*, 211−219.
(36) (a) www.ktechnano.com (accessed May 31, 2012). (b) www.ntmdt-tips.com (accessed May 31, 2012)
(37) (a) Randin, J. P.; Yeager, E. *J. Elechochem. Soc.* **1971**, *778*, 711−714. (b) Randin, J. P.; Yeager, E. J. *Electroanal. Chem.* **1972**, *36*, 257−276. (c) Randin, J. P.; Yeager, E. *J . Electroanal. Chem.* **1975**, *58*, 313−322.
(38) Bard, A. J.; Faulkner, L. R. *Electrochemical methods: fundamentals and applications*, 2nd ed.; John Wiley & Sons: New York, 2001.
(39) (a) Konopka, S. J.; McDuffie, B. *Anal. Chem.* **1970**, *42*, 1741−1746. (b) Aoki, K.; Akimoto, K.; Tokuda, K.; Matsuda, H.; Osteryoung, J. *J. Electroanal. Chem.* **1984**, *171*, 219−230.
(40) (a) Birkin, P. R.; SilvaMartinez, S. *J. Electroanal. Chem.* **1996**, *416*, 127−138. (b) Macpherson, J. V.; O'Hare, D.; Unwin, P. R.; Winlove, C. P. *Biophys. J.* **1997**, *73*, 2771−2781.
(41) (a) Bowling, R.; Packard, R. T.; McCreery, R. L. *Langmuir* **1989**, *5*, 683−688. (b) Bowling, R. J.; McCreery, R. L.; Pharr, C. M.; Engstrom, R. C. *Anal. Chem.* **1989**, *61*, 2763−2766.
(42) (a) Hathcock, K. W.; Brumfield, J. C.; Goss, C. A.; Irene, E. A.; Murray, R. W. *Anal. Chem.* **1995**, *67*, 2201−2206. (b) Alsmeyer, D. C.; McCreery, R. L. *Anal. Chem.* **1992**, *64*, 1528−1533. (c) Alliata, D.; Häring, P.; Haas, O.; Kötz, R.; Siegenthaler, H. *Electrochem. Commun.* **1999**, *1*, 5−9.
(43) Tamayo, J.; Garcia, R. *Langmuir* **1996**, *12*, 4430−4435.
(44) (a) López-Palacios, J.; Heras, A.; Colina, A.; Ruiz, V. *Electrochim. Acta* **2004**, *49*, 1027−1033. (b) Pharr, C. M.; Griffiths, P. R. *Anal. Chem.* **1997**, *69*, 4673−4679.
(45) (a) Colley, A. L.; Williams, C. G.; D'Haenens Johansson, U.; Newton, M. E.; Unwin, P. R.; Wilson, N. R.; Macpherson, J. V. *Anal. Chem.* **2006**, *78*, 2539−2548. (b) Wilson, N. R.; Clewes, S. L.; Newton, M. E.; Unwin, P. R.; Macpherson, J. V. *J. Phys. Chem. B* **2006**, *110*, 5639−5646.
(46) (a) Banerjee, S.; Sardar, M.; Gayathri, N.; Tyagi, A. K.; Raj, B. *Phys. Rev. B* **2005**, *72*, 075418−075424. (b) Lu, Y.; Muñoz, M.; Steplecaru, C.; Hao, C.; Bai, M.; Garcia, N.; Schindler, K.; Esquinazi, P. *Phys. Rev. Lett.* **2006**, *97*, 076805−076808. (c) Shvets, V. V.; Sinitsyna, O. V.; Meshkov, G. B.; Yaminsky, I. V. *Mosc. U. Phys. B+* **2010**, *65*, 501−505.
(47) Liu, Y.; Freund, M. S. *Langmuir* **2000**, *16*, 283−286.
(48) (a) Guëll, A. G.; Ebejer, N.; Snowden, M. E.; Macpherson, J. V.; Unwin, P. R. *J. Am. Chem. Soc.* **2012**, *134*, 7258−7261. (b) Patten, H. V.; Lai, S. C.; Macpherson, J. V.; Unwin, P. R. *Anal. Chem.* **2012**, *84*, 5427−5432. (c) Lai, S. C.; Dudin, P. V.; Macpherson, J. V.; Unwin, P. R. *J. Am. Chem. Soc.* **2011**, *133*, 10744−10747.
(49) (a) McCreery, R. L. In *Electroanalytical Chemistry*; Bard, A. J., Ed.; Dekker: New York, 1991; Vol. *17*, pp 221−374. (b) McDermott, M. T.; Kariuki, J. K. *Langmuir* **1999**, *15*, 6534−6540.
(50) (a) Moore, R. R.; Banks, C. E.; Compton, R. G. *Anal. Chem.* **2004**, *76*, 2677−2682. (b) Banks, C. E.; Compton, R. G. *Anal. Sci.* **2005**, *21*, 1263−1268.
(51) Nair, R. R.; Sepioni, M.; Tsai, I. L.; Lehtinen, O.; Keinonen, J.; Krasheninnikov, A. V.; Thomson, T.; Geim, A. K.; Grigorieva, I. V. *Nat. Phys.* **2012**, *8*, 199−202.
(52) Ugeda, M. M.; Brihuega, I.; Guinea, F.; Gomez-Rodriguez, J. M. *Phys. Rev. Lett.* **2010**, *104*, 096804.
(53) Ebejer, N.; Schnippering, M.; Colburn, A. W.; Edwards, M. A.; Unwin, P. R. *Anal. Chem.* **2010**, *82*, 9141−9145.